



Research article

UDC 624:691.34

DOI: 10.34910/MCE.113.1



## Rubber concrete beams under the action of transverse bending

A.V. Levchenko , A.E. Polikutin 

Voronezh State Technical University, Voronezh, Russian Federation

✉ [Alevchenko@vgasu.vrn.ru](mailto:Alevchenko@vgasu.vrn.ru)

**Keywords:** concretes, polymers, rubber, strength, reinforced concrete, concrete construction, finite element method, rubcon

**Abstract.** Bending elements made of rubber polymer concrete (rubcon), which was invented at the Department of Reinforced Concrete and Stone Constructions of the Voronezh Civil Engineering Institute, are a promising direction in the development of the construction industry for industrial buildings due to their high load-bearing capacity combined with universal resistance to aggressive environments. One of the primary building materials today is cement concrete, despite its disadvantages associated with the complexity of the maintenance of reinforced concrete structures in aggressive environments. The previous research on rubcon bending elements of the rectangular cross-section was carried out without implementing numerical studies that consider the nonlinear properties of the materials. Based on the conducted physical experiments, a deformation model of the resistance of the normal cross-sections to the action of transverse bending is developed, which allows estimating the strength of rubcon beams with the greatest deviation of 18%. The accepted prerequisites in the calculation model allow a more correct description of the deformation of polymer concrete in reinforced structures. The proposed analysis method is validated by numerical studies in the ANSYS® software. Due to the obtained excellent convergence with experimental values, physical studies can be replaced by numerical studies.

**Funding:** The experimental studies have been carried out using the facilities of the Collective Research Center named after Professor Yu.M. Borisov, Voronezh State Technical University, which is partly supported by the Ministry of Science and Education of the Russian Federation, Project No 075-15-2021-662.

**Acknowledgments:** We would like to express gratitude to professors Potapov and Figovskiy for scientific advice.

**Citation:** Levchenko, A.V., Polikutin, A.E. Rubber concrete beams under the action of transverse bending. Magazine of Civil Engineering. 2022. 113(5). Article No. 11301. DOI: 10.34910/MCE.113.1

### 1. Introduction

In this study, we consider bending elements made of rubber polymer concrete (rubcon) invented at the Department of Reinforced Concrete and Stone Constructions of the Voronezh Civil Engineering Institute. The optimal composition of the polymer concrete was obtained by prof. Potapov and Figovskiy [1, 2]. It was somewhat optimized later to obtain the best deformation characteristics [3].

One of the primary building materials today is concrete, despite its disadvantages associated with the complexity of using this material in conditions different from residential and civil housing construction without special protective measures, which can be corrected by polymers introduced directly into the concrete composition. The pioneers in the creation of polymer concrete are Oster-Volkov and Itinsky, who obtained a sample of polymer concrete based on furfural acetone monomer in 1956. Further, in 1961-1962, studies of these polymer concretes were carried out at Voronezh Institute of Civil Engineering, Moscow Institute of Transport Engineers and other organizations, on the basis of which the "Guide for the design

and use of structures made of reinforced polymer concrete in construction" was developed, while abroad recommendations for the design of polymer concrete structures are reflected in ACI 548 documents, including recommendations for the selection of compositions, and also in the work of prof. Figovsky [4]. Authors propose, in addition to the existing methods for calculating polymer concrete structures, to take into account the pre-fracture zone above the crack tip since, as the theory of fracture mechanics shows, at the crack tip, stresses that exceed the limiting ones arise. A similar assumption is put forward for reinforced concrete elements, which is stated in [5], while the additional consideration of the zone of extreme deformation above the crack seems relevant, especially in polymer concrete elements due to the greater ductility compared to traditional cement concrete and higher maximum stresses corresponding to the ultimate tensile strength compared to traditional cement-based concrete.

Polymer materials used as a binder have a rather high cost; therefore, in the manufacture of concretes based on them, it is necessary to strive to reduce the consumption of polymer, obtaining effective materials with filler and aggregate content up to 90–95% of the mass. It is important to note that with such a small consumption of polymer binder (less than 10% of the mass); polymer concretes have high strength characteristics and high chemical resistance. Due to the presence of a large volume of production of synthetic rubbers on the territory of the Russian Federation, their use as a binder in the manufacture of polymer concrete is of practical interest.

The study of the properties of rubber concrete was carried out by the authors of [1, 2, 6], based on which its physical and mechanical parameters and their dependence on variations in compositions were established. A distinctive feature of this material is its high chemical resistance. In the article [7] Borisov obtained and analyzed the coefficients of chemical resistance by for environments that are found in industrial enterprises of various kinds. Chmykhov, in his dissertation work, somewhat expanded the boundaries of this study, thereby proving that rubcon has universal resistance to particularly aggressive media, for example, its chemical resistance coefficient in water is 1. Rubber concrete has high tensile strength, while the modulus of elasticity corresponds to heavy concretes of the class B25-B30, which is an undoubted advantage in comparison with most of the currently known polymer concretes [4], [8]. Which indicates the promising use of rubcon as a material for the manufacture of bending structures. The study of structures made of rubber concrete was carried out by the authors [9–11], including reinforced-rubcon bending T-section elements [11]. Research on reinforced concrete elements with a 5 mm thick rubber concrete coating was carried out by Pinaev in order to provide protection from an aggressive environment [9]. There were also works on the study of a double-layered bending structure with a rubcon in a tensile zone and with ordinary concrete in the compressed zone [10], where it was established that the strength of the "rubcon-concrete" joint is higher than the shear strength of concrete. In the study of rectangular beams [12], it was found that the ultimate strength of inclined sections is achieved when deflections are higher than the maximum permissible, which indicates the expediency of studying the work of normal sections of rubcon beams under load. In view of the presence of fly ash in the rubcon composition, it should be noted that its influence on the strength characteristics and durability was also studied in concretes based on polyester resins [13], as a result of which the effectiveness of its application was proved to reduce the cost of the material. In a separate group of studies, we would like to single out studies of beams made of geopolymer concrete [14]. This type of concrete does not use cement in its composition [15], like most polymer concretes, which is also an advantage because about 7% of the world's greenhouse gases are formed during the production of cement gases [16] and about 1 ton of CO<sub>2</sub> per 1 ton of cement [17]. Among the set of properties of rubcon, it is also worth highlighting high adhesion to materials of various types. Based on research described in the dissertation of Pinaev, it was determined that the adhesion value of the rubcon, for example to a surface made of steel, is 0.8 R<sub>kt</sub> (almost 9.0 MPa) for comparison adhesion value for the ordinary cement concrete is less than 1.0 MPa. Some properties of the rubcon are given in Table 1.

**Table 1. Physical and mechanical properties of rubcon.**

Properties	Indicators for rubcon
Compressive strength, MPa	70...80
Tensile strength, MPa	9...11
Elastic modulus, MPa	24000
Poisson's ratio	0.25-0.26
Shrinkage, mm / m	0.0

Numerical modeling in software packages allow to reduce or completely avoid physical experiments on structural and non-structural components. This direction is especially interesting in the study of innovative (non-traditional) materials. To date, many works are devoted to the problems of studying structures in such software systems as Midas®, ANSYS® and others, while the vast majority of works,

including experimental ones, are devoted to structures made of traditional materials, such as steel or cement concrete [18], recently, composite reinforcement and carbon fiber lamellas have been added to this list [19]. As for polymer concretes, the bulk of research is focused on epoxy and polyester polymer concretes [13], [20].

It is important to note that at the moment, the study of rubcon bending elements of the rectangular cross-section was carried out without the implementation of numerical studies that take into account the nonlinear properties of materials [3, 10-12]. Based on experimental studies, it is necessary to develop a deformation model that will allow to evaluate the strength of normal sections of rubcon beams. Implement a finite element model in ANSYS® that takes into account the nonlinear properties of the material, allow to expand the boundaries of the study, change the size and shape of the cross-section, and reduce the number of field experiments conducted. To do this, we need to determine the actual strength characteristics of the reinforcement and polymer concrete used, as well as to assess the adequacy of the finite element model in comparison with the experiments conducted.

## 2. Methods

### 2.1. Theoretical studies

The prerequisites for the method for calculating the strength of normal sections of rubcon bending elements, which differ from the traditional method for calculating the strength, are based on the analysis of their stress-strain state, established on the basis of physical experimental studies and the information published in [3], [10], [21].

In view of the greater ductility and higher maximum stresses at the ultimate strength of rubber concrete in comparison with the regular cement concrete, it is proposed to include in the calculation the forces from the resistance of polymer concrete to crack propagation, i.e. taking into account the formation of a zone of plastic deformation above the crack tip.

Thus, the following prerequisites of the method for calculating the strength of normal sections of rubcon bending elements were established:

1. The sections above the crack tip remain plane after deformation and are perpendicular to the curved axis of the beam;
2. The calculation is carried out according to the stage of destruction ;
3. The compressed zone stresses are determined from a multilinear deformation diagram. The compressive stress-strain diagram has a nonlinear outline;
4. The part of the rubcon above the crack resists tensile forces;
5. The stresses in the tensile reinforcement during the destruction of the beam do not exceed the yield strength;
6. Inelastic deformations in the tensile zone of concrete at the crack tip are modeled by the pre-fracture zone, which is considered in the work of Irwin [22]. The pre-fracture zone means an area equal to two radii of plasticity at the crack tip in which the stresses at the crack tip tend to have values higher than the ultimate strength of the material.

The distribution of the calculated internal forces and deformations in the normal section of a bending element made of rubber concrete, taking into account the above prerequisites, is shown in Figure 1.

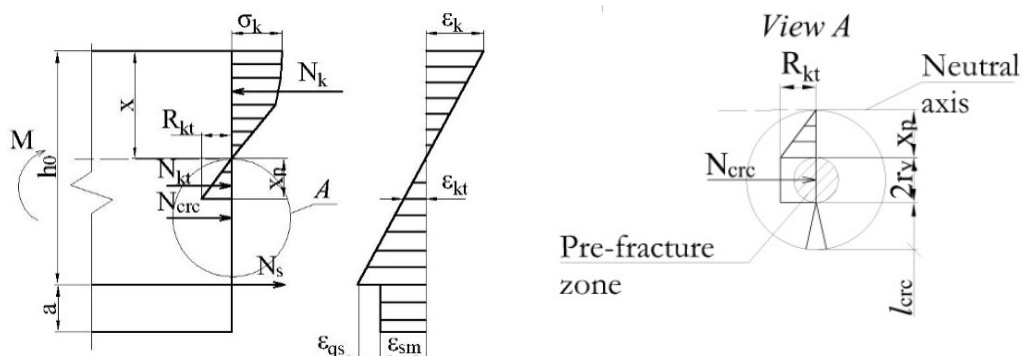


**Figure 1. Distribution of calculated internal forces in a normal section.**

The force in the reinforcement is determined by the formula:

$$N_s = \sigma_s \cdot A_s, \quad (1)$$

where  $A_s$  is rebar area;

$\sigma_s$  are rebar stresses:

$$\sigma_s = \frac{\varepsilon_k (h_0 - x)}{x} E_s, \quad (2)$$

$E_s$  is elastic modulus.

The force in the rubcon tensile zone is determined by the formula:

$$N_{kt} = \frac{1}{2} R_{kt} \cdot x_p \cdot b, \quad (3)$$

where  $x_p = \frac{\varepsilon_{kt}}{\varepsilon_k} x$ ;

$\varepsilon_{kt}$  are tensile rubcon strains;

$\varepsilon_k$  are relative compressive rubcon strains;

$R_{kt}$  is tensile strength;

$b$  is section width.

The force in the rubcon compressed zone is determined by the formula:

$$N_k = \omega \cdot \sigma_k \cdot x \cdot b, \quad (4)$$

where  $\omega$  is the coefficient of completeness of the compressed zone epure, obtained on the basis of the established parameters of the multilinear diagram (Figure 2):

$$\omega = \begin{cases} 0.5 & \varepsilon_k \leq \varepsilon_{k1} \\ 1 - 0.5 \frac{\sigma_{k1} \varepsilon_{k1}}{\sigma_k \varepsilon_k} - \left( \frac{\sigma - \sigma_{k1}}{\sigma} \right) \cdot \left( \frac{\varepsilon_{k1}}{\varepsilon_k} + 0.5 \cdot \left( 1 - \frac{\varepsilon_{k1}}{\varepsilon_k} \right) \right) & \varepsilon_{k1} < \varepsilon_k < \varepsilon_{k0} \\ 1 - 0.5 \frac{\sigma_{k1} \varepsilon_{k1}}{\sigma_k \varepsilon_k} - \left( \frac{\sigma - \sigma_{k1}}{\sigma} \right) \cdot \left( \frac{\varepsilon_{k1}}{\varepsilon_k} + 0.5 \cdot \left( \frac{\varepsilon_{k0} - \varepsilon_{k1}}{\varepsilon_k} \right) \right) & \varepsilon_{k0} \leq \varepsilon_k \leq \varepsilon_{k2} \end{cases} \quad (5)$$

$\sigma_k$  is the maximum compressed zone stress determined from a multilinear diagram, which is obtained from testing of control samples (Figure 2);  $\sigma_{k0}$ ,  $\sigma_{k1}$ ,  $\sigma_{k2}$  are compressive stresses at various stages of loading and  $\varepsilon_{k0}$ ,  $\varepsilon_{k1}$ ,  $\varepsilon_{k2}$  are relative compressive strains at different stages of loading.

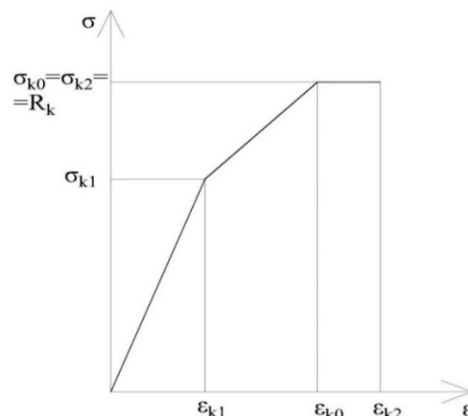


Figure 2. Multilinear stress-strain diagram of rubcon.

Resistance to crack propagation is determined taking into account the J.R. Irwin's correction to the plastic zone above the crack tip [23]:

$$N_{crc} = 2 \cdot r_y \cdot R_{kt} \cdot b, \quad (6)$$

where  $r_y$  is the radius of the plastic zone at the crack tip, determined from the solution of the following system of equations:

$$\begin{cases} K_{IC} = k_0 \cdot R_{kt} \cdot \sqrt{r_y} \\ K_{IC} = R_{kt} \cdot \sqrt{\pi l_{crc}} \\ 2r_y = h_0 - x - x_p - l_{crc} \end{cases} \quad (7)$$

$K_{IC}$  is the critical value of the stress intensity factor;

$k_0$  is empirical coefficient according to [23];

$l_{crc}$  is crack height.

As a result, it was found that the radius of the plastic zone at the crack tip is:

$$r_y = \gamma \cdot h_0 - \gamma \cdot x \left(1 + \frac{\varepsilon_{kt}}{\varepsilon_k}\right), \quad (8)$$

where  $\gamma = \left(\frac{\pi}{k_0^2}\right) / \left(\frac{2\pi}{k_0^2} + 1\right)$ .

The compressed zone height is determined from the sum of the projections of the internal forces on the longitudinal axis of the element:

$$\omega \cdot \sigma_k \cdot x \cdot b - \frac{1}{2} R_{kt} \cdot \frac{\varepsilon_{kt}}{\varepsilon_k} \cdot x \cdot b - \varepsilon_k \cdot E_s \cdot \frac{(h_0 - x)}{x} \cdot A_s - 2R_{kt} \cdot b \cdot \gamma \cdot h_0 + 2R_{kt} \cdot b \cdot \gamma \cdot \left(1 + \frac{\varepsilon_{kt}}{\varepsilon_k}\right) \cdot x = 0. \quad (9)$$

We transform this equation to find the height of the compressed zone:

$$A \cdot x^2 + B \cdot x - \varepsilon_k \cdot h_0 \cdot E_s \cdot A_s = 0, \quad (10)$$

$$\text{where } A = \omega \cdot \sigma_k \cdot b - \frac{1}{2} R_{kt} \cdot \frac{\varepsilon_{kt}}{\varepsilon_k} \cdot b + 2R_{kt} \cdot b \cdot \gamma \cdot \left(1 + \frac{\varepsilon_{kt}}{\varepsilon_k}\right) = 0, \quad (11)$$

$$B = \varepsilon_k \cdot E_s \cdot A_s - 2R_{kt} \cdot b \cdot \gamma \cdot h_0. \quad (12)$$

The bending moment is determined from the equilibrium of moments of all internal forces relative to the center of gravity of the tensioned rebar:

$$M_u = N_k \cdot (h_0 - y_t) - N_{kt} \cdot \left(h_0 - x - \frac{2}{3} x_p\right) - N_{crc} \cdot (h_0 - x - x_p - r_y), \quad (13)$$

where  $y_t = S_{red} / A_{red}$  – the center of gravity of the stress diagram of the compressed zone.

## 2.2. Experimental studies

To study normal sections of reinforced rubcon beams of rectangular cross-section, experimental specimens with longitudinal bar reinforcement were manufactured and tested for pure bending. Reinforcing bars were grade A500C and B500 per GOST 34028-2016. The percentage of longitudinal reinforcement varied in the range from 0.8% to 6.3%. Beams in the experiment were designed as the beams, which failure starts with the reinforcement reaching its yield stress.

The tests were carried out at the Center for Collective Use (CCU) of the Voronezh State Technical University, Russia. The beams were loaded with two equal concentrated loads applied vertically in thirds of the span. With this type of load application, the value of the bending moment arising in the beam

increases from zero at the support to the maximum value under the point of load application. Between the points of application of the load, the shear force is zero, and the value of the bending moment is constant and equal to the maximum value - the zone of pure bending. The diagram of load application on specimen-beams and their reinforcement are shown in Figure 3. Beam-samples were tested on a laboratory press "INSTRON 600KN" (60 tons). The tests were carried out at a constant speed; the movement of the press traverse was 1 mm/min.

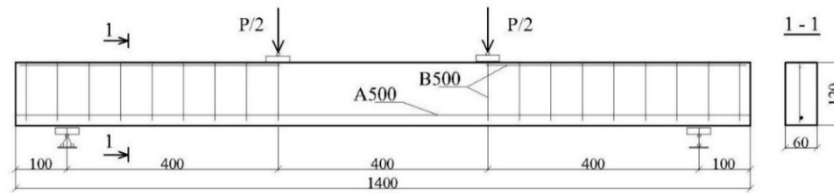


**Figure 3. Loading scheme, section and reinforcement of bending elements.**

To study the stress-strain state of normal sections, strain gauges were glued along the height of the beam section (Figure 4).

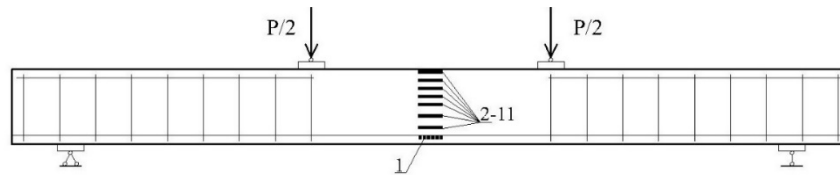


**Figure 4. Strain gauges scheme.**

Strain gauge № 1 for measuring the deformation of the reinforcing bar, strain gauges №2-11 to measure the strain on the section height. The value of the ultimate load was taken as the maximum value of the press force, indicated by the force sensor, at which the yield strength of the reinforcement is reached. Figure 5 shows a general view of a ready-to-test beam installed to a testing machine.



**Figure 5. General view of the beam BRR-2x14 prepared for testing.**

With each series of beams, three concrete prism samples and three rebar samples were tested to determine the compressed strength of concrete and rebar mechanical properties. Reinforcing bars were grade A500 per GOST 34028-2016. Based on the test results, the actual strength characteristics of the materials were obtained (Table 2) and used in the calculations. Table 2 also shows the values of the ultimate bending moment and the height of the compressed and tensile zones.

**Table 2. Test results.**

Beam designation	Reinforcement percentage $\mu, \%$	$R_k$ , MPa	$\sigma_y$ , MPa	$M_u^e$ , kNm	$x^e$ , mm	$x_p^e$ , mm
BRR - 1x8	0.8	81	565	2.96	32	22
BRR - 1x10	1.25	81	600	4.28	38	18
BRR - 1x12	1.8	80	600	5.80	46	16
BRR - 2x10	2.5	75	600	7.82	44	16
BRR - 2x12	3.6	79	600	10.30	61	15
BRR - 2x14	4.95	79	635	14.00	62	11
BRR - 2x16	6.3	80	550	15.32	60	10

*Note: Beam designation BRR-NxM means that rectangular beams are made of rubcon, N – number of reinforcing bars, M – diameter of reinforcing bars.  $M_u^e$  is ultimate bending moment according to test results;  $x^e$ ,  $x_p^e$  are height of compressed and tensile zones according to test results.*

### 2.3. The FEM simulations

ANSYS® software package was used for finite element analysis of rubcon beams using nonlinear properties of materials. On the right support of the beam, a roller was set, prohibiting only vertical displacements, but allowing all rotations and horizontal displacements. A pinned support was set on the left side. The length of the support zone was 60 mm, the cantilevers of the beam were 75 mm. Two concentrated forces act on the beam, located similar to the test scheme (Figures 6 and 7).

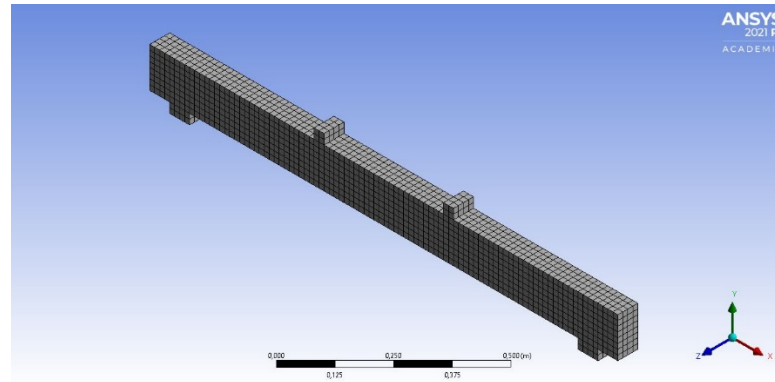


Figure 6. Finite element model of the element under research.

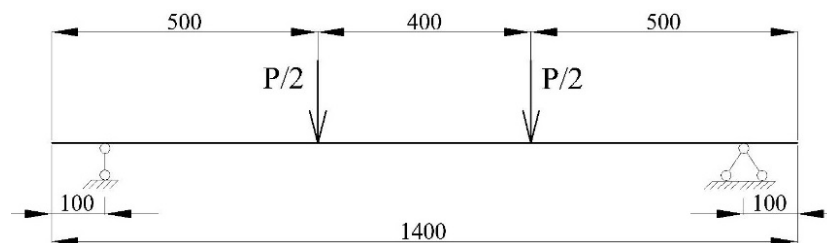


Figure 7. Design scheme of the element under research.

The eight nodal finite element Solid65 was used to model concrete. This element type is capable of simulating plastic deformations, cracking in tension and crushing in compressed. This finite element implements the “Willam-Warnke” concrete deformation model [24]. The model includes the following parameters: the stress-strain relationship for compression, elastic modulus  $E_k$ , compressive strength  $R_k$  and tensile strength  $R_{kt}$ , Poisson's ratio  $\nu$ , shear transfer coefficient for closed and open cracks  $\beta_t$  and  $\beta_c$ . To model the longitudinal and transverse reinforcement, the finite element Beam 188 was used, which is a linear spatial finite element. The support and load plates have a thickness of 20 mm and are made of steel, the contact zone is rigid. The mesh size of the finite element model was chosen in such a way that the nodes of the rod element modeling the reinforcement bar match with the nodes of the solid elements to ensure a rigid contact between the polymer concrete body and the reinforcement.

To describe the mechanical characteristics of polymer concrete, a multilinear diagram of the relationship between stress and strain is used, which is shown in Figure 2,  $\varepsilon_{k1} = 0.2\%$ ,  $\sigma_{k1} = 48.0$  MPa, this point means that the beginning of microcracking occurs,  $\varepsilon_{k0} = 0.45\%$ , this point means that the beginning of macrocracking occurs,  $\varepsilon_{k2} = 0.55\%$ ,  $\sigma_{k0} = \sigma_{k2} = 80.0$  MPa. For the rubcon, the coefficient of transfer of shear forces for closed cracks,  $\beta_t$ , is taken equal to 0.4, for open cracks,  $\beta_c$ , 0.9 in accordance with [25], [26].

For A500 rebar and B500 transverse rebar, bilinear stress-strain diagrams were used. The first parametric point is the elastic limit, the second is the limit of plastic deformation, which was taken as 2.5%.

The mechanical characteristics of the B500 rebars are taken in account with the normative documents (Russian State Standard GOST 34028-2016). The relative longitudinal deformations of the first point are  $\varepsilon_{s0} = 0.25\%$ . The stress values for the first and second points are taken equal to  $\sigma_y$ , the yield point = 500 MPa. When modeling bars, the relative longitudinal deformations of the second point are  $\varepsilon_{s2} = 2.5\%$ . The stress-strain relationship are assumed to be identical for tension and compression. The diagrams are taken ignoring hardening beyond the yield point.

### 3. Results and Discussion

Figure 8 shows the results of vertical displacements of the BRR–2x12 beam under the action of a load, obtained experimentally and according to the results of finite element analysis.

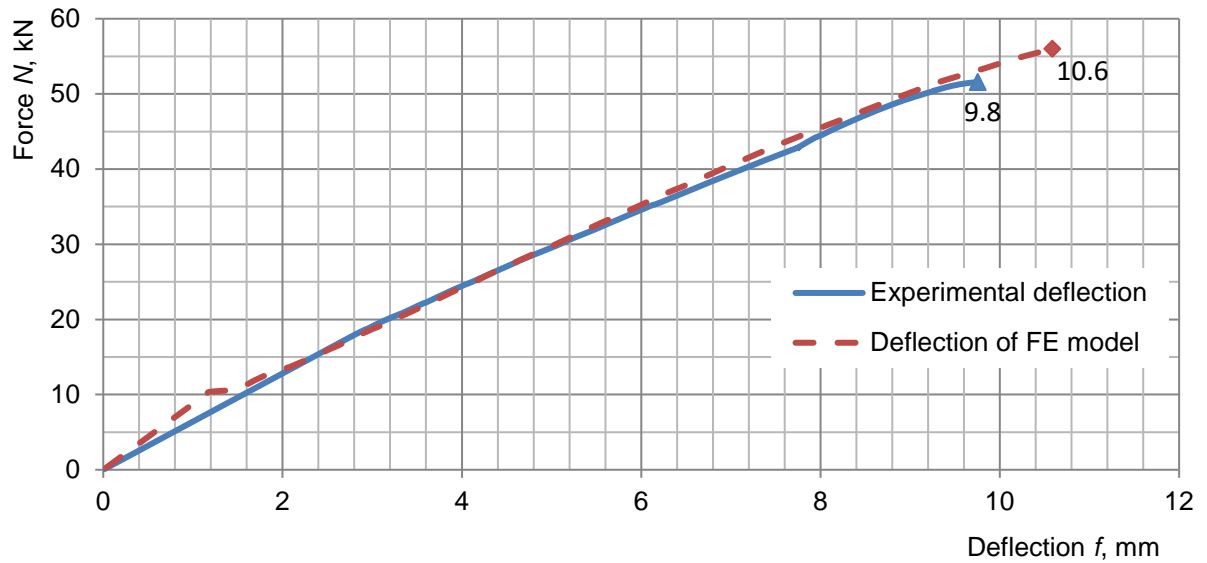


Figure 8. Deflection of a beam with  $\mu = 3.6\%$  reinforcement.

This indicates an excellent convergence of the experiment and the FE model, but Figure 9 shows the results of the stress distribution over the height of the section located in the middle of the span. From which it can be seen that the value of the height of the tensile concrete above the crack is lower than in the experimental samples.

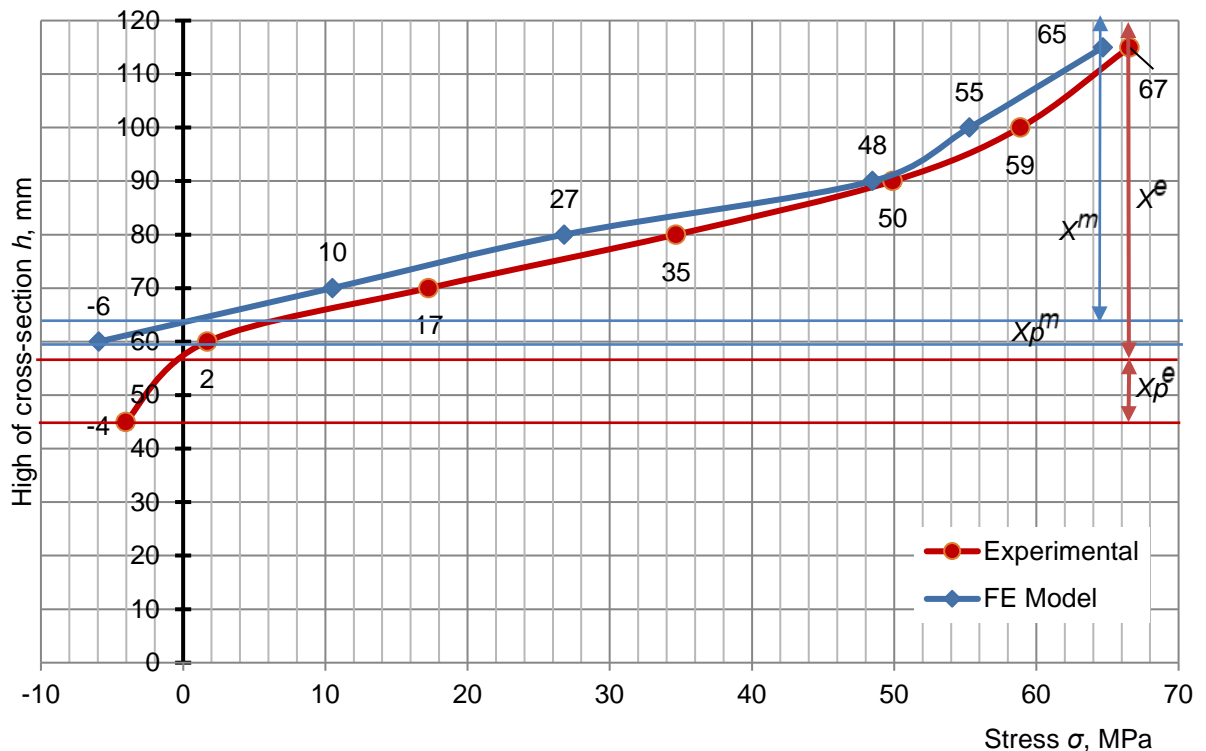


Figure 9. Normal stresses in cross-section of beam with  $\mu = 3.6\%$  reinforcement at failure.



Figures 10-15 show a general view of the model of the beam and the reinforcement at failure.

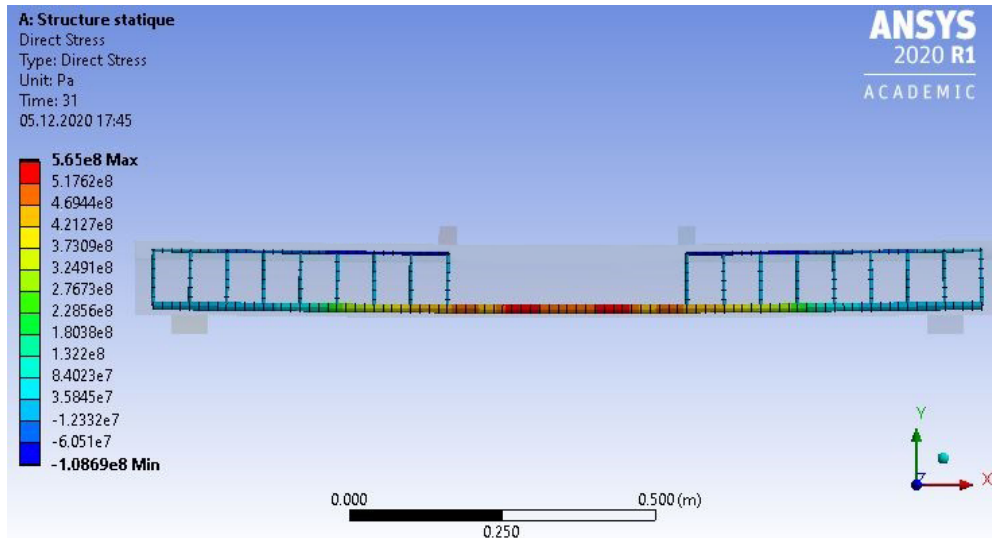


Figure 10. Normal stresses in reinforcement in the FE model of a beam with  $\mu = 0.8\%$  reinforcement at failure.

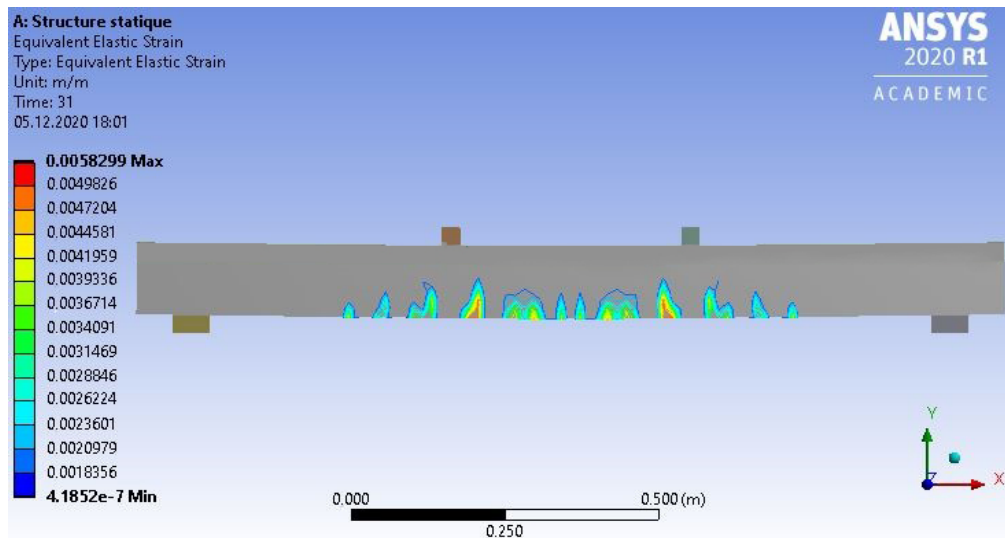


Figure 11. Development of elastic strain (cracks) in the FE model of a beam with  $\mu = 0.8\%$  reinforcement at failure.

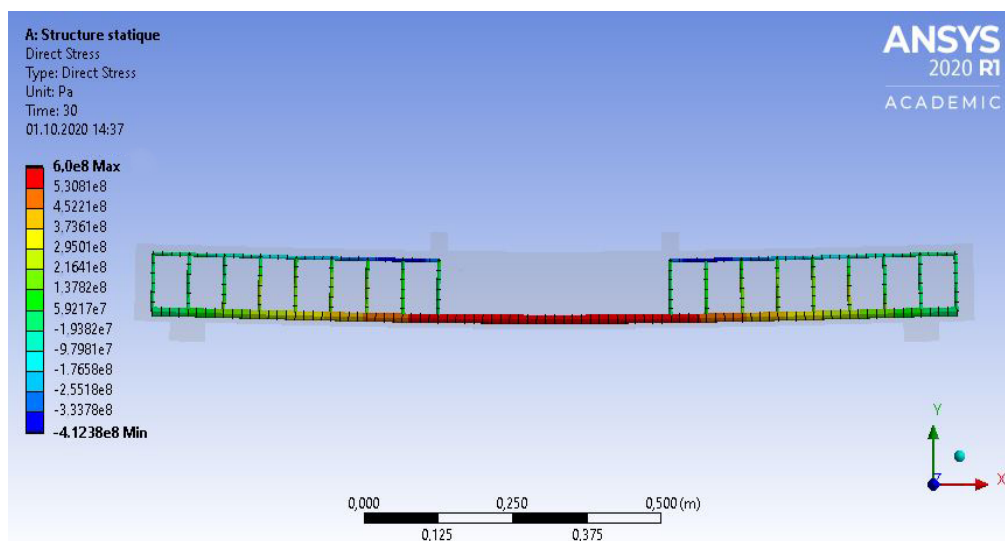


Figure 12. Normal stresses in reinforcement in the FE model of a beam with  $\mu = 3.6\%$  reinforcement at failure.

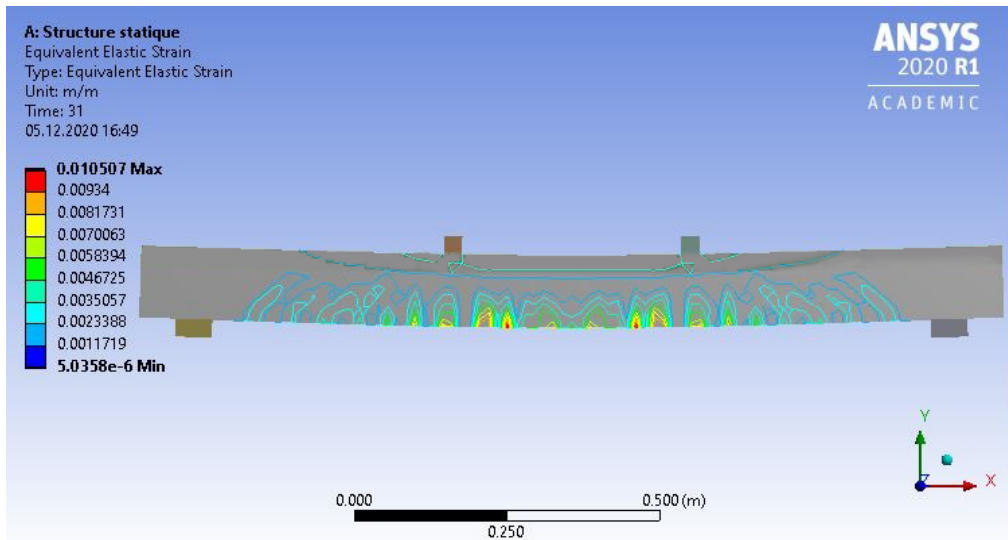


Figure 13. Development of elastic strain (cracks) in the FE model of a beam with  $\mu = 3.6\%$  reinforcement at failure.

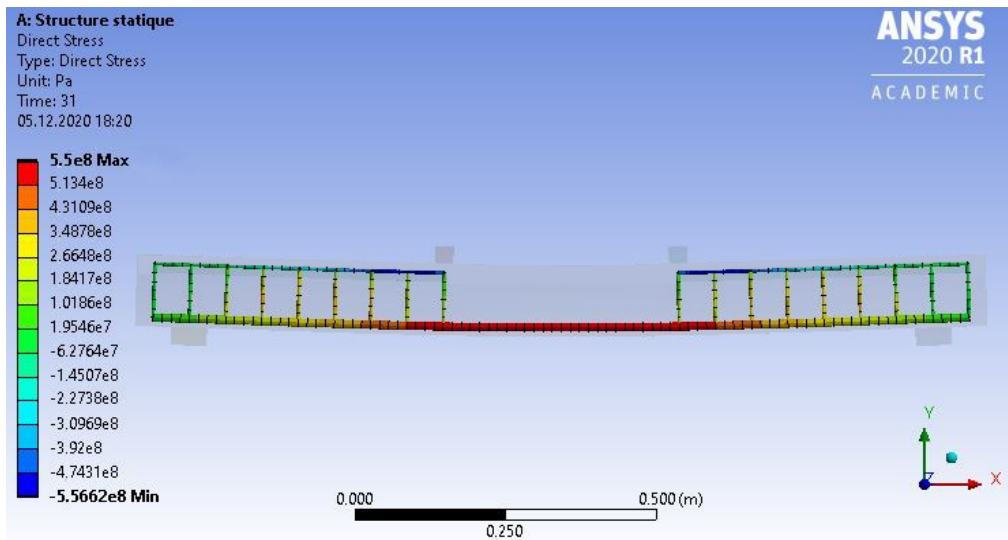


Figure 14. Normal stresses in reinforcement in the FE model of a beam with  $\mu = 6.3\%$  reinforcement at failure.

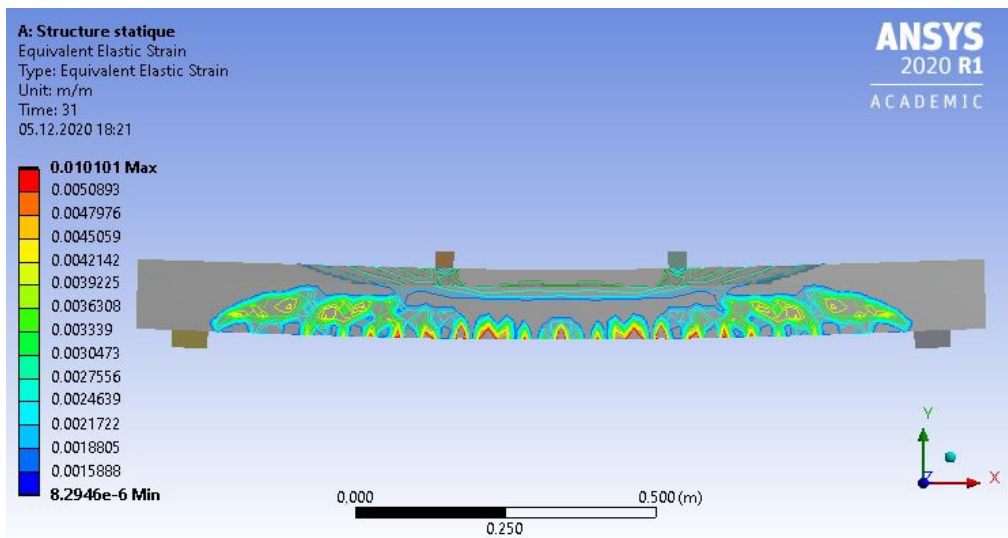


Figure 15. Development of elastic strain (cracks) in the FE model of a beam with  $\mu = 6.3\%$  reinforcement at failure.

It is obvious that the general picture of the FE model of the beam before failure with an increase in the percentage of reinforcement corresponds to the logic of failure of bending elements, i.e. the model shows the appearance and development of a larger number of areas of development of elastic strains (cracks). Also, according to Figures 8 and 9, it can be argued about the adequacy and good convergence of the data obtained from the results of finite element analysis.

The results of the carried out theoretical, experimental and numerical studies of rubcon bending elements are summarized in Table 4.

**Table 4. Research results.**

Beam designation	Reinforcement percentage $\mu, \%$	$M_u^t$ , kNm	$M_u^m$ , kNm	$M_u^e$ , kNm	$\Delta M_u^t$ , %	$\Delta M_u^m$ , %
BRR - 1x8	0.8	2.51	2.60	2.96	-18.0	-13.8
BRR - 1x10	1.25	4.02	4.20	4.28	-6.6	-1.9
BRR - 1x12	1.8	5.82	6.00	5.80	0.4	3.3
BRR - 2x10	2.5	7.92	8.00	7.82	1.3	2.3
BRR - 2x12	3.6	10.86	11.20	10.30	5.2	8.0
BRR - 2x14	4.95	14.47	15.20	14.00	3.3	7.9
BRR - 2x16	6.3	14.96	16.80	15.32	-2.4	8.8

Note:  $M_u^t$  is ultimate bending moment according to the design results according to the proposed method;  $M_u^m$  is ultimate bending moment according to the results of design in ANSYS®;  $\Delta M_u^t$  is deviation of calculation results according to the proposed method from experimental values;  $\Delta M_u^m$  is deviation of calculation results in ANSYS® from experimental values.

The relationship between the ultimate bending moment and the percentage of longitudinal reinforcement is shown in Figure 16.

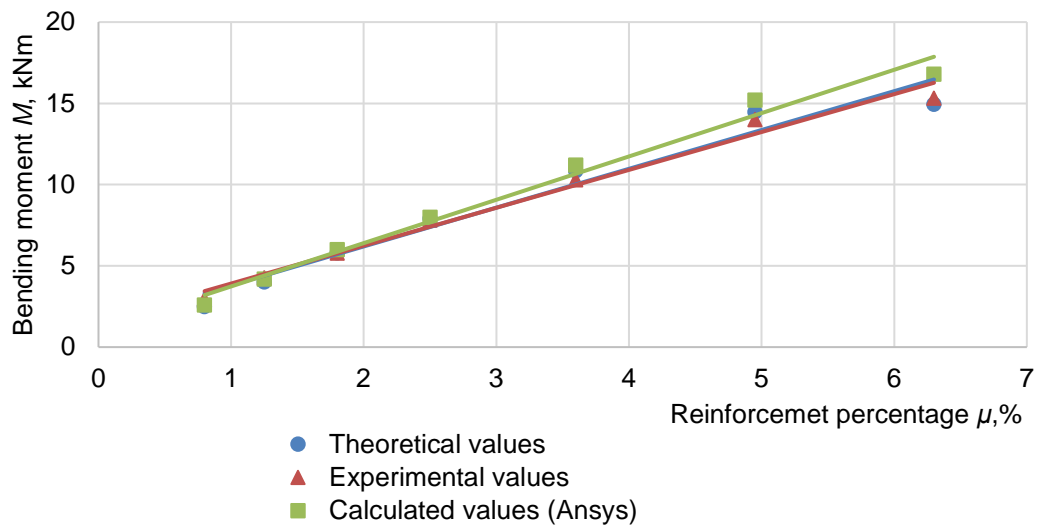


**Figure 16. Relationship between the ultimate bending moment and reinforcement percentage.**

Table 5 shows the values of the heights of the compressed and tensile zones of concrete above the crack, as well as the values of the height of the tensile zone calculated without taking into account the accepted prerequisite. Table 6 shows the deviations of the values of Table 5 from the experimental.

**Table 5. Height of compressed and tensile zones.**

Beam designation	$x^t$ , mm	$x_p^t$ , mm	$x^e$ , mm	$x_p^e$ , mm	$x^m$ , mm	$x_p^m$ , mm	$x_p$ , mm
BRR - 1x8	39	22.5	32	22	32.5	17.5	14.2
BRR - 1x10	41	19.2	38	18	40	15	11.9
BRR - 1x12	45	16.6	46	16	42.5	15	10.1
BRR - 2x10	51	14.7	44	16	52.5	10	8.9
BRR - 2x12	57	12.3	61	15	55	7.5	7.4
BRR - 2x14	63	10.2	62	11	6,5	7.5	6.1
BRR - 2x16	67	9.8	60	10	72.5	7.5	6.4

**Table 6. Value of deviation from experimental data.**

Beam designation	$\Delta x^t, \%$	$\Delta x_p^t, \%$	$\Delta x^m, \%$	$\Delta x_p^m, \%$	$\Delta x_p, \%$
BRR - 1x8	-22.6	-2.1	-1.6	20.5	35,5
BRR - 1x10	-9.0	-6.2	-5.3	16.7	33,9
BRR - 1x12	1.4	-3.4	7.6	6.3	36,9
BRR - 2x10	-15.3	8.7	-19.3	37.5	44,4
BRR - 2x12	6.1	21.8	9.8	50.0	50,7
BRR - 2x14	-2.3	8.0	-4.8	31.8	44,5
BRR - 2x16	-12.0	2.4	-20.8	25.0	36,0

Note:  $x^t, x_p^t$  are height of compressed and tensile zones according to the design results according to the proposed method;  $x^m, x_p^m$  is height of compressed and tensile zones according the results of design in ANSYS®;  $\Delta x^t, \Delta x_p^t$  are deviation of calculation results according to the proposed method from experimental values;  $\Delta x^m, \Delta x_p^m$  are deviation of calculation results in ANSYS® from experimental values;  $\Delta x_p$  is deviation of calculation results without taking into account the pre-fracture zone from experimental values.

As can be seen from Table 6, the most correctly values of the height of the tensile concrete zone are determined according to the method developed by the author.

The above assumptions of the calculation are confirmed by the studies in the article [5], which indicate the need to take into account the pre-fracture zone when calculating reinforced concrete elements in the stage of exploitation, as well as studies of the stress-strain state of rubber concrete bending elements of rectangular section [3], and T-section [11]. In order to reduce the cost of manufacturing beams, the authors of [9] propose to use a "cage" made of rubber polymer concrete, however, this method will significantly increase the resistance of the structure to environmental influences and only slightly the bearing capacity and crack resistance. To increase the load-bearing capacity and reduce the cost of rubcon beams, in [10], studies of a two-layer bending element with a rubcon only in the tensile zone were carried out, but now these studies were carried out only in the experimental stage without implementation of software packages.

Approach implemented with FE modeling of rubcon beams, as described above, was tested in [25] for calculating the reinforced concrete elements and the calculating the concrete elements reinforced by CFRP lamellas [26] and showed excellent agreement with experimental data.

From the analysis of Figure 16, it can be said that the proposed method for calculating the strength of normal sections provides excellent convergence with the experimental values (the largest deviation is 18.0% in the series of beams BRR-8). Application of ANSYS® software allows to adequately perform a numerical strength analysis (the largest deviation is 13.8% towards the margin in the series of BRR-8 beams, the smallest deviation is 1.9% in the series of BRR-10 beams). Consequently, the strength calculation method proposed in this work provides sufficient convergence with experimental values and is confirmed by theoretical and numerical studies.

The accepted prerequisites in the calculation model allow to more correctly describe the deformation of polymer concrete in reinforced structures.

## 4. Conclusion

1. Rubber concrete beams are competitive in the construction industry in terms of their strength characteristics in combination with chemical resistance.
2. The proposed method for calculating the strength of normal sections provides excellent convergence with experimental values.
3. A comparison of the results of theoretical, numerical and experimental studies showed that the "Willam-Warnke" theory for composite materials, implemented in the ANSYS® software with the application of the established characteristics of materials, allows to calculate the strength of rubcon beams.
4. The conducted experimental studies can be replaced by numerical studies.

## References

1. Figovsky, O. New polymeric matrix for durable concrete. Proceedings of the International Conference on Cement Combinations for Durable Concrete. 2005. DOI: 10.1680/ccfdc.34013.0029.
2. Figovsky, O., Beilin, D., Blank, N., Potapov, J., Chernyshev, V. Development of polymer concrete with polybutadiene matrix. Cement and Concrete Composites. 1996. 18(6). DOI: 10.1016/S0958-9465(96)00036-4.

3. Polikutin, A., Potapov, Y., Levchenko, A., Perekal'skiy, O. The Stress-Strain State of Normal Sections Rubcon Bending Elements with Mixed Reinforcement. *Advances in Intelligent Systems and Computing*. 2019. 983. DOI: 10.1007/978-3-030-19868-8\_56.
4. Figovsky, O., Beilin, D. *Advanced polymer concretes and compounds*. 2013.
5. Iakovenko, I.A., Kolchunov, V.I. The development of fracture mechanics hypotheses applicable to the calculation of reinforced concrete structures for the second group of limit states. *Journal of Applied Engineering Science*. 2017. 15(3). DOI: 10.5937/jaes15-14662.
6. Potapov, Yu.B., Chmykhov, V.A., Borisov, Yu.M. Resistance of a polymer concrete based on polybutadiene binder to organic and inorganic acids. *Scientific Israel - Technological Advantages*. 2013. 15 (4). Pp. 7–10.
7. Potapov, Yu. B., Borisov, Yu. M. Wear-Resistant Coatings On The Basis Of Oligodienes. *Russian Journal Of Building Construction And Architecture*. 2010. No. 1. Pp. 38–44.
8. Bedi, R., Chandra, R., Singh, S.P. Reviewing some properties of polymer concrete. *Indian Concrete Journal*. 2014. 88(8).
9. Potapov, Y.B., Pinaev, S.A., Arakelyan, A.A., Barabash, A.D. Polymer-cement material for corrosion protection of reinforced concrete elements. *Solid State Phenomena*. 2016. 871. DOI:10.4028/www.scientific.net/MSF.871.104.
10. Borisov, Yu. M., Polikutin, A. E., Nguen Phan Duy. The Stress-strain state of normal sections of double-layered, rubcon-concrete bending elements of building structures. *Russian Journal Of Building Construction And Architecture*. 2011. No. 2. Pp. 6–13.
11. Potapov, Y. Polikutin, A. Panfilov, D. Okunev, M. Comparative analysis of strength and crack resistance of normal sections of bent elements of T-sections, made of rubber concrete, caoutchouc reinforcement and concrete. *MATEC Web of Conferences*. 2016. No. 73. DOI:10.1051/mateconf/20167304018.
12. Borisov, Y.M., Polikutin, A.E. Strength of inclined sections of bendable reinforcing elements. *Beton i Zhelezobeton*. 2004. (1).
13. Gorninski, J.P., Dal Molin, D.C., Kazmierczak, C.S. Comparative assessment of isophthalic and orthophthalic polyester polymer concrete: Different costs, similar mechanical properties and durability. *Construction and Building Materials*. 2007. 21(3). DOI: 10.1016/j.conbuildmat.2005.09.003.
14. Ahmed, H.Q., Jaf, D.K., Yaseen, S.A. Flexural Capacity and Behaviour of Geopolymer Concrete Beams Reinforced with Glass Fibre-Reinforced Polymer Bars. *International Journal of Concrete Structures and Materials*. 2020. 14(1). DOI: 10.1186/s40069-019-0389-1.
15. Kar, A., Ray, I., Halabe, U.B., Unnikrishnan, A., Dawson-Andoh, B. Characterizations and Quantitative Estimation of Alkali-Activated Binder Paste from Microstructures. *International Journal of Concrete Structures and Materials*. 2014. 8(3). DOI: 10.1007/s40069-014-0069-0.
16. Mehta, K. Reducing the Environmental Impact of Concrete. *Concrete international*. 2001.
17. Radhakrishna, Venu Madhava, T., Manjunath, G.S., Venugopal, K. Phenomenological Model to Re-proportion the Ambient Cured Geopolymer Compressed Blocks. *International Journal of Concrete Structures and Materials*. 2013. 7(3). DOI: 10.1007/s40069-013-0048-x.
18. Najafgholipour, M.A., Arabi, A.R. Finite-Element Study on the Behavior of Exterior Reinforced Concrete Beam-to-Column Connections with Transverse Reinforcement in the Joint Panel. *Practice Periodical on Structural Design and Construction*. 2021. 26(1). DOI: 10.1061/(asce)sc.1943-5576.0000537.
19. Mansour, W. Numerical analysis of the shear behavior of FRP-strengthened continuous RC beams having web openings. *Engineering Structures*. 2021. 227. Pp. 111451. DOI:10.1016/j.engstruct.2020.111451.
20. Lokuge, W., Aravinthan, T. Effect of fly ash on the behaviour of polymer concrete with different types of resin. *Materials and Design*. 2013. 51. DOI: 10.1016/j.matdes.2013.03.078.
21. Zhurtov, A. V., Khezhev, T.A., Mailyan, D.R. Analysis of the Stress-Strain State of Two-Layer Reinforced Cement Structures. *Proceedings of the 2018 International Conference "Quality Management, Transport and Information Security, Information Technologies", IT and QM and IS 2018*. 2018. DOI: 10.1109/ITMQIS.2018.8525119.
22. Irwin, G.R. Plastic zone near a crack and fracture toughness. *7th Sagamore Ardance Materials Research Conference*. 1960.
23. Peresypkin, E.N. Raschyot sterzhnevnyh zhelezobetonnyh elementov [Calculation of reinforced concrete core elements]. 1988. (rus)
24. Willam, K.J., Warnke, E.P. Constitutive Model for the Triaxial Behaviour of Concrete. *IABSE Proceedings, Vol 19*. 1975.
25. Mostofinejad, D., Talaeitaba, S.B. Nonlinear modeling of RC beams subjected to torsion using the smeared crack model. *Procedia Engineering*. 2011. 14. DOI:10.1016/j.proeng.2011.07.182.
26. Hii, A.K.Y., Al-Mahaidi, R. An experimental and numerical investigation on torsional strengthening of solid and box-section RC beams using CFRP laminates. *Composite Structures*. 2006. 75(1–4). DOI:10.1016/j.compstruct.2006.04.050.

### **Information about authors:**

#### **Artem Levchenko**

ORCID: <https://orcid.org/0000-0002-6875-754X>

E-mail: [Alevchenko@vgasu.vrn.ru](mailto:Alevchenko@vgasu.vrn.ru)

#### **Aleksei Polikutin, PhD in Technical Science**

ORCID: <https://orcid.org/0000-0001-7280-5746>

E-mail: [a.pl@mail.ru](mailto:a.pl@mail.ru)

*Received 06.03.2021. Approved after reviewing 19.11.2021. Accepted 24.11.2021.*